

1 Variability of Black Carbon mass concentration in surface snow at Svalbard

2 Michele Bertò^{1#}, David Cappelletti^{2,7}, Elena Barbaro^{1,3}, Cristiano Varin¹, Jean-Charles Gallet⁴, Krzysztof
3 Markowicz⁵, Anna Rozwadowska⁶, Mauro Mazzola⁷, Stefano Crocchianti², Luisa Poto^{1,3}, Paolo Laj⁸,
4 Carlo Barbante^{1,3} and Andrea Spolaor^{1,2*}.

5
6 ¹Ca' Foscari University of Venice, Dept. Environmental Sciences, Informatics and Statistics, via Torino,
7 155 - 30172 Venice-Mestre, Italy;

8 ²Università degli Studi di Perugia, Dipartimento di Chimica, Biologia e Biotecnologie, Perugia, Italy;

9 ³CNR-ISP, Institute of Polar Science – National Research Council –via Torino, 155 - 30172 Venice-
10 Mestre, Italy;

11 ⁴Norwegian Polar Institute, Tromsø, Norway.

12 ⁵University of Warsaw, Institute of Geophysics, Warsaw, Poland;

13 ⁶Institute of Oceanology, Polish Academy of Sciences, Sopot, Poland;

14 ⁷CNR-ISP, Institute of Polar Science – National Research Council – Via Gobetti 101, Bologna;

15 ⁸Univ. Grenoble-Alpes, CNRS, IRD, Grenoble-INP, IGE, 38000 Grenoble, France

16

17 [#] Now at Laboratory of Atmospheric Chemistry, Paul Scherrer Institute, 5232 Villigen PSI, Switzerland

18

19 Correspond to: Andrea Spolaor, andrea.spolaor@cnr.it; Michele Bertò, michele.berto@gmail.it

20

21 Abstract

22 Black Carbon (BC) is a significant forcing agent in the Arctic, but substantial uncertainty remains
23 to quantify its climate effects due to the complexity of the different mechanisms involved, in particular
24 related to processes in the snowpack after deposition. In this study, we provide detailed and unique
25 information on the evolution and variability of BC content in the upper surface snow layer during the
26 spring period in Svalbard (Ny-Ålesund). Two different snow-sampling strategies were adopted during
27 spring 2014 (from April 1st to June 24th) and during a specific period in 2015 (April 28th to May 1st),
28 providing the *refractory* BC (rBC) mass concentration variability on a seasonal/daily and daily/hourly
29 time scales. The present work aims to identify which atmospheric variables could interact and modify the
30 mass concentration of BC in the upper snowpack, the snow layer which BC particles affects the snow
31 albedo. Atmospheric, meteorological, and snow-related physical-chemical parameters were considered in
32 a multiple linear regression model to identify the factors that could explain the variations of BC mass

33 concentrations during the observation period. Precipitation events were the main drivers of the BC
34 variability during the seasonal experiment however in the high resolution sampling a negative association
35 have been found. Snow metamorphism and activation of local sources (Ny-Ålesund was a coal mine
36 settlement) during the snow melting periods appeared to play a non-negligible role. The statistical
37 analysis suggests that the BC content in the snow is not directly associated to the atmospheric BC load.

38 1. Introduction

39 In the last two decades, the Arctic region has been exposed to dramatic changes in terms of
40 atmospheric temperature rise, sea ice decrease, and increase of air mass transport from lower latitudes
41 bringing warmer and humid air masses containing pollutants and anthropogenic derived compounds (Law
42 and Stohl, 2007; Comiso et al., 2008; Screen and Simmonds, 2010; Eckhardt et al., 2013; Schmale et al.,
43 2018; Maturilli et al., 2019). Long-range transport and local emissions of combustion generating aerosols
44 like black carbon (BC) can influence the radiative budget of the Arctic atmosphere, especially the impacts
45 of atmospheric aging on the mixing state of BC particles (Eleftheriadis et al., 2009; Bond et al., 2013;
46 Zanatta et al., 2018). When deposited over snow, numerous aerosol species directly increase the quantity
47 of solar radiation absorbed by the snowpack, thus favouring snow aging processes and the decrease of the
48 snow albedo (Hansen and Nazarenko, 2004; Flanner et al., 2007; Hadley and Kirchstetter, 2012; Skiles et
49 al., 2018; Skiles and Painter, 2019).

50 Among these light-absorbing aerosols, *black carbon* (BC) particles are the most effective in
51 absorbing the visible and near infrared solar radiation. These primarily emitted, insoluble, refractory and
52 carbonaceous particles originate from natural and anthropogenic sources such as open fires or diesel
53 engine exhausts. Currently, the anthropogenic emissions are higher compared to the natural ones
54 (Moosmüller et al., 2009; Bond et al., 2013). In 2000, the energy production sector (including fossil fuels
55 and solid residential fuels combustion) generated approximately 59% of the total global BC emissions
56 while the remaining came from biomass burning (Bond et al., 2013). BC particles are characterized by a
57 mass size distribution peaking around 100-250 nm (or mass equivalent diameter), e.g. 240 nm in the
58 Svalbard area in spring (Bond et al., 2013; Laborde et al., 2013; Zanatta et al., 2016; Motos et al., 2019).
59 The impact of BC particles absorbing the incoming solar radiation has indeed a non-negligible role in the
60 Arctic region, which is already threatened by a two-fold temperature increase compared to the mid-
61 latitude areas, the so-called “Arctic Amplification” (Bond et al., 2013; Cohen et al., 2014; Serreze and
62 Barry, 2011). BC has an atmospheric lifetime of about seven days and has been directly targeted in
63 important international mitigation agreements (AMAP, 2015). Theoretical and experimental results
64 showed that the cryosphere is affected both by the BC-induced warming of the atmosphere and by direct
65 and indirect BC effects on the snow once deposited over it (Flanner, 2013),

66 Atmospheric BC measurements in the Arctic regions are still rare, despite an extraordinary effort
67 done by the international scientific community to evaluate the sources, transport paths, concentration, and
68 climate impact (Eleftheriadis et al., 2009; Pedersen et al., 2015; Ferrero et al., 2016; Ruppel et al., 2017;
69 Osmont et al., 2018; Zanatta et al., 2018; Laj et al., 2020). BC mass concentrations can be directly
70 measured by using incandescent or thermal techniques and indirectly, by absorption measurements using
71 an appropriate mass absorption cross-section (Petzold, 2013). Various terms such as refractory black
72 carbon (rBC) for incandescent measurements, elemental carbon (EC) using thermal techniques, or
73 equivalent black carbon (eBC) based on optical technique are used. Forsström et al. (2009) reported
74 measurements performed in Arctic snow in the past and new measurements of EC in snow surface using
75 filters and a thermo-optical method. The geographical and seasonal eBC variability was investigated in
76 the Arctic region by Doherty et al. (2010). Other BC measurement in snow samples from the Arctic
77 region can be found in Aamaas et al. (2011), Forsström et al. (2013), Pedersen et al. (2015), Gogoi et al.
78 (2016), Khan et al. (2017) and Mori et al. (2019). Intercomparison of different techniques agree within a
79 factor of 2 uncertainty at Alert (Sharma et al., 2017), Ny-Ålesund, and Barrow (Sinha et al., 2017).

80 A complex combination of processes are involved in the BC particles transfer from the
81 atmosphere to the surface snow. Via a modelling approach, Liu et al. (2011) found that approximately
82 50% of BC's total burden in the Arctic atmosphere is removed through wet deposition-related processes.
83 Yasunari et al. (2013) estimated the intensity of BC dry deposition on the Himalayan glaciers; they found
84 that the surface roughness and the surface wind speed are critical parameters in order to retrieve realistic
85 results. In a recent study, Jacobi et al. (2019) confirmed the previous estimates suggesting that
86 approximately 60% of the BC particles are deposited on the surface snow via wet deposition in spring in
87 the Svalbard Arctic area. Models are still not fully able to describe the actual deposition and transport
88 processes in Svalbard, resulting in underestimating the BC concentration in the snowpack (Eckhardt, S. et
89 al 2015, Stohl, A. et al. 2013). Although wet deposition is suggested to be the main driver of BC
90 concentration in the snow, little is known about other environmental processes potentially affecting the
91 BC particles concentration once deposited, i.e. physical post-depositional processes.

92 In this study we present two unique experiments performed in a clean area close to the town of
93 Ny-Ålesund (Svalbard) at the Gruvebadet Aerosol Laboratory (78.91734 N, 11.89535 E, 40 m a.s.l.),
94 during spring 2014 and 2015. Daily and hourly time resolution samplings were performed on the snow
95 surface to investigate which atmospheric variables could directly or indirectly modify the BC mass
96 concentration in the surface snow once deposited. The daily sampling lasted for approximately 85 days to
97 assess the intra-seasonal variability covering the transition from a cold period (April) to the melting
98 period in late June. The hourly time resolution experiment was performed to investigate the existence of
99 potential processes affecting the BC concentration over the diurnal cycle.

100
101
102
103
104
105
106
107
108
109
110
111
112
113
114
115
116
117
118
119
120
121
122
123
124
125
126
127
128
129
130
131
132
133

2. Experimental Methods

2.1 Study Area

Both experiments were conducted in the proximity of the Ny-Ålesund research station (78.5526 N, 11.5519 E, 25 m a.s.l.), located on the Spitzbergen Island in Svalbard archipelago. Along the west coast, Svalbard is characterized by a maritime climate with an annual average temperature of -3.9°C in Ny-Ålesund (between 1994 and 2017) (Maturilli et al., 2019). On average, the snowpack starts building up in September and melts away at the end of May (Førland et al. 2011). Ny-Ålesund has become one of the reference locations for conducting Arctic climate studies focusing on atmospheric composition and physics. Long-term monitoring of atmospheric aerosols is performed at the Gruvebadet station (Feltracco et al., 2019, 2020, 2021a, 2021b; Moroni et al., 2018; Ferrero et al., 2016; Bazzano et al., 2015; Moroni et al., 2015; Zangrando et al., 2013; Scalabrin et al., 2012, Turetta et al., 2021), and at the Zeppelin observatory (475 m a.s.l.) (Eleftheriadis et al., 2009; Tunved et al., 2013; Lupi et al., 2016, and reference therein).

2.2 Snow Sampling

There are no standardized methods for sampling, filtering and analytical protocols for detecting atmospheric carbon deposited in snow, even if a few protocols have been developed (Ingersoll et al., 2009; Gallet et al., 2018; Meinander et al., 2020). In the present work, two different sampling strategies were adopted regarding the thickness of the sampled layer and the temporal sampling frequency.

Snow samples were collected during two field campaigns: The first campaign was carried out in Spring 2014, from April 1st to June 24th for a total of 85 days, it consists of daily sampling and it is referred hereafter as the “85-days experiment”. The second campaign was conducted in Spring 2015 from April 28th to May 1st. During these three days, measurements were collected with hourly sampling. This second campaign is hereafter referred as the “3-days experiment”. Snow samples were collected about 1 km North-West of Ny-Ålesund (Figure 1). The area is a dedicated clean site for aerosols and snow sampling, with no fuel engine traffic. The wind at the site is usually blowing from east to west, and rarely from North to South, minimizing the emission of the town reaching the sampling area. The main wind pattern during the experiment is presented in Figures 1 and 2. The samples for both experiments were kept frozen until the lab analyses. The samples were collected using neck nylon gloves to avoid any contamination.

The two experiments aim to capture the rBC mass concentration on a daily basis in the surface snow (upper 10 cm) during the seasonal change and on an hourly basis on a thinner surface snow layer (upper 3 cm) during a daily cycle. Although wet and dry deposition are the main sources of BC in the

134 Artic snow, the aim of our experiments was to evaluate if other atmospheric parameters could contribute
135 to the snow surface rBC mass concentration variability.

136 In the 85-days experiment, the first 10 cm of surface snow were collected on a daily basis
137 (approximately at 11.00 am, GMT+2) in the same area, using a 5 cm diameter and 10 cm long Teflon
138 tube. The samples were collected following a straight line leaving about 15 cm between the sampling
139 points to minimize the spatial variability. The collected snow was homogenized in a pre-cleaned plastic
140 bag and then, without melting, 50 mL was transferred into vial (Falcon™ 50mL Conical Centrifuge
141 Tubes) for BC, coarse mode particles number (mix of soil, mineral coarse mode and possibly coal coarse
142 mode) concentration and electrical conductivity analyses. The 85-days experiment was designed with the
143 aim to investigate the BC presence in the upper snow layer, where most of the snow-radiation interaction
144 takes place and where BC particles' presence can decrease the snow albedo (Doherty et al., 2010). Snow
145 albedos increased rapidly and asymptotically as the snow depth increased. Visible albedos reached 0.9 for
146 a snow depth of only 5 cm (Perovich et al. 2007). Moreover, this sampling strategy allowed to evaluate
147 the variation of BC on a seasonal basis and to capture the impacts of wind, precipitation or melting.

148 During the 3-days experiment, the first 3 cm of surface snow were collected on an hourly basis in
149 pre-cleaned vials in a delimited area of 2 x 2 m using the same sampling tools as above (Spolaor et al.,
150 2019). In this case the samples were collected following a straight line leaving about 5 cm between the
151 sampling points. The aim of the 3-days experiment was to investigate the potential daily cycle of surface
152 BC concentration; therefore, we foresaw that small variations could derive from the impact of the daily
153 variation of short-wave radiation (SWR) and subsequent induced snow metamorphism at the surface of
154 the snowpack, often at cm scale. To avoid dilution of the signal, we reduced the vertical sampling
155 thickness to 3 cm to enhance our chances of observing variation in the rBC mass concentration, if such
156 variation exists.

157 The temperature at the surface of the snowpack (at 7 cm for 85-days and at 3 cm for 3-days
158 experiment) was always measured. The daily/hourly snow accumulation was determined by measuring
159 the emerging part of 4 poles placed around the sampling area. The average standard deviation calculated
160 from the four poles provides us a reasonable estimate of the variability in snow accumulation\depletion
161 within the sampling area. The standard deviation obtained ranges from 2 to 4 cm for the entire periods,
162 indicating a limited spatial variability.

163

164 **2.3 Atmospheric Optical Measurements**

165 **2.3.1 Aethalometer (AE-31)**

166 In this study, the equivalent BC (eBC) concentration in the Boundary Layer (around 3 m a.s.l.)
167 was measured by an AE-31 aethalometer (Gundel et al., 1983), during the 3-day campaign. The device is

168 equipped with 7-wavelengths (370, 470, 520, 590, 660, 880, 950 nm). It determines the attenuation
169 coefficient by using the light attenuation ratio through a sensing spot and a referenced clean spot, both on
170 a quartz fiber filter substrate. The sampling and reference spots surface areas are 0.5 cm^2 , while the
171 volumetric flow rate is 4 L min^{-1} . The flow rate was calibrated with a TetraCal (BGI Instruments)
172 volumetric airflow before and after the field campaign. A 5 minutes temporal resolution was used for data
173 acquisition. However, due to the low background concentration in the Arctic, the signal/noise ratio is
174 high, so that data were hourly averaged. The data presented in this study were processed according to
175 Segura et al. (2014) methodology. For this purpose the multiple scattering and filter loading effect
176 (Weingartner et al., 2003) was corrected with new values of mass absorption cross section (MAC) and
177 multiple scattering factor ($C=3.1$), reported by Zanatta et al. (2018). The MAC value was derived using
178 observations and observationally constrained Mie calculations in spring at the Zeppelin Arctic station
179 (Svalbard, 78°N). Zanatta et al. (2018) estimated the MAC at 550 nm ($9.8 \text{ m}^2 \text{ g}^{-1}$) and at 880 nm (6.95 m^2
180 g^{-1}), which we used to estimate MAC at 520 nm ($10.2 \text{ m}^2 \text{ g}^{-1}$).

181

182 **2.3.2 Particle Soot Absorption Photometer (PSAP)**

183 During the 85-days sampling period the aerosol absorption coefficient was also measured by
184 means of a 3-wavelengths PSAP (this instrument was not available during the 3-days experiment period).
185 It measures the variation of light transmission through a filter where particles are continuously deposited
186 with constant airflow. A second filter identical to the first one remains clean and is used as a reference to
187 take into account possible variations of the light source, i.e. a 3-color LED (blue, green and red with
188 wavelength centred around 470, 530 and 670 nm, respectively). The correction developed by Bond et al.
189 (1999) was applied to consider the filter loading effect. The complete eBC mass concentration time series
190 for the 85-days experiment was retrieved using the Aethalometer (first period) and the PSAP (second
191 period), with an overlapping period with simultaneous measurements of 5 days. For the retrieved eBC
192 mass concentration from the two instruments to be equal during the overlapping period, the PSAP eBC
193 was calculated dividing the absorption measurements (at 530 nm) with a MAC equal to $7.25 \text{ m}^2 \text{ g}^{-1}$
194 (keeping the AE31 data as reference). Daily averages were calculated from the 1-minute data to compare
195 with the rBC daily data obtained from the snow.

196

197 **2.4 Surface Snow measurements**

198 **2.4.1 Coarse Mode Particles Number Concentration**

199 The snow samples were melted at room temperature before the on-line coarse-mode particles and
200 conductivity measurements (the water was pumped from the vials by a 12 channels peristaltic pump,
201 ISMATECH, type ISM942). **The total conductivity of the melted snow was measured in parallel with a**

202 **simple conductivity Micro-Cell**. The number concentration of coarse mode particles in the surface snow
203 was measured with a Klotz Abakus laser sensor particle counter. This instrument optically counts the total
204 number of particles and measures each particle's size in a liquid constantly flowing through a laser beam
205 cavity (LDS 23/23). The measurements size range of the instrument is from 0.8 to about 80 μm with 32
206 dimensional bins (Table SI 1), not overlapping with that of the SP2. Only the 32nd bin has a dimensional
207 range above 15.5 μm , i.e. of 80 μm . The data were recorded by a LabView® based software obtaining a
208 sufficient number of data points in order to have a standard deviation less than 5% of the mean value. The
209 particles number concentration was calculated using the constant water flow value.

210

211 **2.4.2 rBC Measurement – SP2**

212 The rBC mass concentration and mass size distribution were measured following the methods
213 described in Lim et al. (2014). The snow samples were melted at room temperature prior to the analyses.
214 The vials with the melted snow were sonicated for ten minutes at room temperature. The samples were
215 nebulized before the injection in the Apex-Q desolvation system (APEX-Q, Elemental Scientific Inc.,
216 Omaha, USA). The nebulization efficiency was evaluated daily by injecting Aquadag® solutions with
217 different mass concentrations, ranging from 0.1 to 100 ng g^{-1} , obtaining an average value of 61%, that
218 was used to correct all the BC mass concentrations reported in this manuscript. More details on the
219 method can be found in Lim et al. (2014) and in Wendl et al. (2014).

220 The SP2 data were analyzed using the IGOR based toolkit from M. Gysel (Laboratory of
221 Atmospheric Chemistry, Paul Scherrer Institute, Switzerland). The large amount of signals derived from
222 every single particle are elaborated achieving rBC mass and number concentrations and size distributions.

223

224 **2.5 Meteorological Parameters**

225 Meteorological parameters, in addition to the atmospheric and snow ancillary measurements,
226 were used in the statistical exercise to study the variability of rBC mass concentration in surface snow
227 samples as a function of the atmospheric conditions. BC particles are deposited on the snowpack
228 following a combination of wet and dry deposition. However, once deposited on/in the snowpack other
229 processes can potentially induced a significant variability in the surface BC content. The wind direction
230 and its velocity can modify the BC distribution in the upper snowpack due to snow-mobilization. The
231 solar radiation and relative humidity may enhance snow sublimation and surface hoar formation thus
232 modifying the relative BC concentration in the upper snow layer by removing or adding “water” mass to
233 the snow surface.

234 Air temperature and relative humidity at 2 meter height have been retrieved from a meteorological station
235 located about 800 meters north of the sampling site, using a ventilated PT-100 thermo-couple by Thies

236 Clima and a HMT337 humicap sensor by Vaisala, respectively. Wind speed and direction at 10 meter
237 height were obtained from a Combined Wind Sensor Classic by Thies Clima (see Maturilli et al., 2013).
238 At about 50 m distance, the radiation measurements for the Baseline Surface Radiatio Network (BSRN)
239 provide among others the downward solar radiation detected by a Kipp&Zonen CMP22 pyranometer
240 (Maturilli et al., 2015). Both meteorological and surface radiation measurements are available in a 1-
241 minute time resolution via the PANGAEA data repository (Maturilli et al., 2020). The daily/hourly mean
242 values of the meteorological parameters were used in the statistical analyses of the 85-days/3-days
243 experiment and in Figures 2 and 3 (the physical-chemical parameters from the snow samples are punctual
244 values).

245

246 **2.6 Parameters considered in the statistical analysis**

247 The snowpack evolution is primarily driven by meteorological parameters, which are responsible for
248 adding/removing mass to the annual snowpack. Wind can affect the snow pack evolution in several ways:
249 1) by snow redistribution, 2) favouring the ablation\sublimation, and 3) lifting particles from nearby
250 sources and areas. Surface snow and air temperatures are two fundamental parameters required to fully
251 understand the varying conditions of the snow pack. In our study, the temperature variables are proxies
252 for the melting episodes and for the presence of liquid water potentially affecting the concentration of
253 impurities. The air and snow temperatures do not have a direct effect in the rBC concertation in surface
254 snow, but they are fundamental indicators to identify the spring warming events ($T > 0^{\circ}\text{C}$, called also the
255 Rain on Snow events - ROS) that yield the snow melting. Moreover, air and snow temperature could be
256 relevant to evaluate possible snow metamorphism and the response of the upper snowpack to the
257 meteorological conditions. Snow and air temperatures can be used during the 3-days experiment to
258 evaluate the daily scale frequency and be helpful to investigate the daily scale variability of rBC in the
259 surface snow.

260 The SWR is not expected to be directly linked to the surface mass concentration of rBC, however the
261 surface process could affect it indirectly by favouring sublimation (water mass removal), as well as hoar
262 formation (water mass addition) during the colder parts of the day (night/early morning). The relative
263 humidity gives an idea of the amount of water present in the atmosphere and the high RH might favour
264 the deposition of BC suspended by the formation of water droplets through the cloud condensation nuclei.
265 This parameter is especially significant for the selected sampling location, nearby to the shore. Indeed,
266 relative humidity values close or higher than 90% could be associated to fog or low cloud conditions and
267 not directly to wet or dry precipitations. The last meteorological parameter considered is the precipitation
268 amount. This aspect is important to understand the wet deposition processes able to transfer BC particles
269 from the atmosphere to the snow surface.

270 The additional selected parameters are 1) the atmospheric eBC mass concentration, to investigate
271 the possible link between eBC particles present in the atmosphere and the rBC in snow surface, 2) the
272 coarse mode particles that could have a similar transport pathways to the black carbon and gives an idea
273 of the amount of total impurities deposition and 3) the total water conductivity, an indirect measurement
274 of the salinity content of the snow. It is important to note that the eBC and the rBC mass concentrations
275 are not the same physical quantities: the former is obtained from an absorption measurement assuming a
276 constant MAC, whereas the second is obtained via a laser-induced-incandescence method with an SP2
277 empirically calibrated with a reference material (Petzold et al., 2013). Considering the location of the
278 sampling site (<1 km from the coastline), the contribution of the ocean emissions to the snowpack
279 chemical composition is significant. We considered the total conductivity as an indication of sea spray
280 deposition, and to investigate common deposition patterns and/or similarities to the behaviour of BC
281 (although BC is not emitted from ocean surface). The conductivity was also considered to determine if
282 there was a large sea-spray aerosol event which could, potentially affecting the SP2 measurements (see
283 supplementary material).

284

285 **2.7 Statistical Analysis**

286 Multiple linear regression was carried out to evaluate the relationship between the observed
287 surface snow rBC mass concentration and the selected set of covariates consisting of the meteorological
288 and snow physical-chemical parameters that could have a direct effect on controlling snowpack dynamics
289 as well on the BC concentration as discussed in Section 2.6. All the atmospheric parameters described in
290 the previous section (wind, snow and air temperature, incoming solar radiation, relative humidity, and
291 snow precipitation amount) were initially considered as covariates to be included in the multiple linear
292 regression. However, wind speed and direction, as well as the atmospheric stability, expressed as vertical
293 wind speed, were removed because preliminary statistical analyses indicate that none of them is
294 associated with the observed variations in snow rBC mass concentrations. This does not mean that such
295 parameters do not play a role in controlling the BC concentration, but that no statistically significant
296 associations were found with the data collected in our study and thus these parameters were no longer
297 considered in the statistical analyses discussed below.

298 Multiple linear regression models were fitted on the logarithm scale because the distribution of rBC
299 concentrations in both experiments is characterized by a significant skewness. Coarse mode particles
300 number concentrations and conductivity were also log-transformed to linearize their relationships with
301 log(rBC). The regression model fitted on the two experiments is

302

$$\log(rBC) = \beta_0 + \beta_1 \log(dust) + \beta_2 eBC + \beta_3 temp + \beta_4 snow + \beta_5 swr + \beta_6 \log(cond) + \epsilon.$$

303
304 In the above model, ‘dust’ indicates coarse mode particles number concentrations, ‘temp’ is the snow
305 temperature at 7 cm depth for the 85-days experiment (daily resolution) and at 2 cm depth for the 3-days
306 experiment (hourly resolution), ‘snow’ is a binary indicator for the presence of solid precipitation, ‘swr’ is
307 solar incoming shortwave radiation, ‘cond’ is the conductivity and ε is a zero-mean normal error.
308 Graphical inspection of residuals plots and normal probability plots confirmed that after the logarithm
309 transformations, the regression models meet the assumptions of linearity, constant error variance (called
310 *homoscedasticity* in the statistical literature) and normal errors. The statistical analyses were performed
311 with the statistical language R (R Core Team, 2020).

312

313 **3. Results and Discussions**

314 **3.1 Seasonal BC variability in surface snow**

315 **3.1.1 Atmospheric eBC and atmospheric condition**

316 During the experimental period, the atmospheric eBC concentration ranged between from 80 ng m^{-3} to <
317 5 ng m^{-3} (Figure 2) with an average of $34 \pm 23 \text{ ng m}^{-3}$. The highest concentrations were measured at the
318 beginning of the campaign, especially from April 15th to 27th, followed by a general decreasing trend
319 characterized by the presence of several concentration peaks (on May 8th, 17th and 24th) potentially due to
320 Eurasian fires, as already suggested from Feltracco et al., 2020 (Figure S1). The ammonia daily
321 concentration time series (the only available biomass burning tracer for that period in the area) measured
322 at the Zeppelin station is plotted together with the Gruebadet atmospheric BC measurements in Figure
323 S3. Biomass burning is a significant source of atmospheric ammonia (Andreae and Merlet, 2001), often
324 affecting the Arctic region (Moroni et al. 2020). As shown in Figure S3, both time series have a similar
325 behaviour at the very beginning of the campaign, from April 3rd to 8th and during the period between May
326 7th and 21st. This suggests that the BC detected in the atmosphere could be originated from biomass
327 burning episodes during these two time periods. During the 85-days sampling period, wind was
328 characterized by the following median values (25th and 75th percentiles) for direction and speed: 205°
329 (152° , 257°) and 2.7 (1.9 , 3.7) m s^{-1} , respectively, therefore mostly coming from south-west (Figure 2).
330 Daily air temperature at 3 m increased during the campaign from -15°C to about $+5^\circ\text{C}$ (Figure 2)
331 following the seasonal variation of incoming solar energy: from 100 to 300 W m^{-2} with an average of 185
332 $\pm 75 \text{ W m}^{-2}$ (Figure 2, orange line). The snow precipitation episodes are presented as daily-accumulated
333 values (Figure 2, blue bars) ranging from zero to 12 cm.

334

335 **3.1.2 Surface Snow Conditions**

336 Over the 85 days experiment, the snow rBC mass concentration varies from 0.2 to 6 ng g⁻¹ (Figure 2),
337 with an average of 1.4 ± 1.3 ng g⁻¹, in agreement with results available in the literature (Mori et al., 2019;
338 Jacobi et al., 2019; Aamaas et al., 2011). An increasing trend can be observed for the rBC mass
339 concentration in the surface snow across the sampling period. The median of the rBC mass equivalent
340 diameter in the snow is 313 ± 35 nm (Figure 2), similar to what obtained in other studies (e.g. Schwarz et
341 al., 2013). The rBC mass equivalent diameter show high variability, ranging from 200 to 500 nm.
342 However, since the rBC concentrations were low, the evaluation of the geometric mean of the particles
343 diameter for the biggest sizes, above 300 to 400 nm, has been considered as qualitative information due to
344 the high signal noise.

345 The number of coarse mode particles (Figure 2, blue line) shows a constant concentration in the first half
346 of the campaign (1st April - May 11th - average concentration of 3435±1824 # ml⁻¹) whereas it increases in
347 the second half (12th of May to 27th of June - average concentration of 7782±5683 # ml⁻¹), especially after
348 the 1st of June (1st of June to 27th of June - average concentration of 9352±6741 # ml⁻¹), in concomitance
349 with the onset of the snow melting period. The conductivity (Figure 2, green line) also shows an
350 increasing trend at the end of the sampling campaign when snow is melting, with an overall average value
351 of 30 ± 8 µS. The spatial variability of rBC, calculated in the same manner as proposed by Spolaor et al.
352 (2019) for other species, was obtained from six surface snow samples collected in the four corners of the
353 sampling area and two surface snow samples in the centre right before the beginning of the experiment.
354 The following rBC mass concentrations were obtained: a) 3.95 ng g⁻¹; b) 4.92 ng g⁻¹ c) 4.20 ng g⁻¹ d) 3.10
355 ng g⁻¹ e) 3.82 ng g⁻¹ f) 3.58 ng g⁻¹, resulting in a rBC spatial variability of 16% in the surface snow of the
356 considered sampling area.

357

358 3.1.3 Statistical Results

359 The fitted multiple linear regression model for the 85-days experiment data explains the 69% of
360 the variance of the logarithm of the snow rBC mass concentration ($R^2 = 0.69$). The fitted model indicates
361 the presence of strongly statistically significant associations of the (log transformed) snow rBC mass
362 concentration with the coarse-mode particles number concentration ($p < 0.001$) and the snow temperature
363 ($p < 0.001$). A weaker association is found with the occurrence of snow precipitations ($p = 0.03$). The
364 statistical associations of rBC mass concentration with the other covariates considered in the model are
365 non-significant. See Table 1 for the estimated coefficients and the corresponding p-values.

366 In order to interpret the statistical results, the description of the 85-days campaign is split into two periods
367 identified as the transition from the “cold” to the “melting” state. The first period occurred before the end
368 of May: the rBC mass concentration often increases with snowfall episodes (April 9th/10th/11th and 17th,

369 May 17th, 22nd and 27th/28th; June 1st) as suggested by previous studies, with exceptions for April 24th and
370 May 7th. Over the sampling period, a weakly statistically significant positive association ($p = 0.03$) was
371 found between snow rBC mass concentration in surface snow and the occurrence of snow precipitations.
372 BC wet deposition processes are estimated to remove 50% - 60% of the total atmospheric BC burden in
373 the Arctic (Liu et al., 2011; Jacobi et al., 2019). In our study, the wet deposition impacts could be partially
374 masked due to the sampling frequency and the wind snow. In Kongsfjord, a strong wind is often present
375 during the precipitation events (Figure 2). Consequently, the freshly deposited snow is frequently
376 removed from the surface before being able to sample it. Interestingly, our observations show that, on a
377 daily scale, the precipitation episodes are not clearly related to a decrease in the atmospheric eBC mass
378 concentration (Figure 2). A possible explanation is that the precipitation amounts were small so that the
379 precipitation events did not significantly alter the atmospheric BC reservoir.

380 In the second period, from the beginning of June, the atmospheric temperature increases, causing the
381 snow-melting season's onset. At the beginning of June, the snow rBC mass concentration increases up to
382 approximately 5 ng g^{-1} , and a simultaneous increase was detected in the coarse mode particles number
383 concentration (peaks between June 4th and 7th). As suggested in previous studies, the surface melting
384 process could explain the observed increase in rBC and coarse mode particles concentrations. However,
385 we also have to consider that rBC can be dry deposited, as it has been recently suggested (up to 50-60%;
386 Liu et al., 2011; Jacobi et al., 2019). Very few field validation data exist for estimating the amount of dry
387 deposition at the snow surface, and this process is often used as an ancillary information since most
388 models underestimate the BC in the Arctic snowpack compared to field measurements.

389 Our data support the hypothesis related to local sources' activation in enhancing the dry deposition
390 impacts in an old mining town as Ny-Alesund. Especially during poor snow cover conditions, as during
391 the snow-melting season, coarse mode particles as residuals of carbon extraction mining activities are
392 available for wind lift/suspension (Vecchiato et al. 2018). The possible effect of local sources' activation
393 is further supported by a recent analysis of the Brøggerbreen glacier and Ny-Ålesund annual snowpack.
394 This analysis shows the presence of retene (an organic compound frequently used to track the presence of
395 coal), most likely due to local sources (Vecchiato et al., 2018).

396 The simultaneous increase of rBC mass and coarse mode particle number concentrations during the
397 second part of the experiment (e.g. visible between June 3rd and June 7th-8th) could be explained via
398 similar post-depositional processes: snow melting and sublimation. The episodes of snow surface melting
399 can significantly affect the snow particulate content and we hypothesize that the hydrophobicity of pure
400 BC particles, and of several species in the coarse mode particles, might affect its physical location in the

401 snowpack (in the literature, the response of the BC particles is still debated): the hydrophobicity of the
402 particles can cause the surface concentration to increase while losing water mass through percolation.
403 This could lead into a positive feedback process: the increase of BC concentration can thus enhance snow
404 sublimation (water evaporation) resulting in a further increase of BC concentration in surface snow, and
405 so on.

406 In this study, the estimated statistical association between snow rBC mass concentration and the daily
407 snow temperature is negative and strongly significant ($p < 0.001$). During the 85-days experiment, we can
408 distinguish two events where the temperature appeared to play a role in the BC concentration. Both of
409 them show an increase in rBC mass concentration during melting/refreezing episodes, in agreement with
410 other studies (Aamaas et al., 2011; Xu et al., 2006; Doherty et al., 2013; Doherty et al. 2016). The first
411 event occurred between May 5th to May 12th and the second event after May 20th, when the proper snow
412 melting began (Figure 2). The first event was characterized by a rapid rise of the daily air temperature
413 (from -6°C to -1°C) in concomitance to a snow precipitation event, followed by a rapid temperature
414 decrease to -6°C . The surface snow (10 cm) mirrored this behaviour, first rising from -6°C to 0°C , and
415 then cooling down to -6°C . During this warm event, the upper snow strata underwent a melting episode
416 with surface water percolation (although limited), making the surface BC concentration to increase. The
417 second event started approximately on May 20th and lasted until the end of the experiment (Figure 2).
418 During this period, the atmospheric temperature increased constantly, and the snowpack started to melt
419 consequently. Moreover, surface BC concentration increased almost continuously from May 25th to its
420 maximum observed on June 6th. Afterward, the upper snow rBC mass concentration tended to decrease
421 following the rapid snowpack decline.

422

423 **3.2 Diurnal variation of rBC in surface snow**

424 **3.2.1 Surface Snow/Atmospheric Aerosol Content and Atmospheric Conditions**

425 The 3-days experiment was performed at the end of April 2015, during the Arctic spring. The
426 samples were collected on an hourly basis over 3 days achieving a high-resolution sampling frequency.
427 The atmospheric concentration of eBC ranged from 2 to 50 ng m^{-3} , decreasing during the sampling period
428 and not showing any particular diurnal pattern (Figure 3). The mean value of the atmospheric eBC mass
429 concentration is $34 \pm 23\text{ ng m}^{-3}$, similar to the average of the 85-days experiment.

430 The surface snow rBC mass concentration undergoes to daily time scale change of surface
431 concentration showing up to 2-fold hourly increases (Figure 3, bottom panel, smoothed dark blue line).
432 rBC mass concentrations of approximately 15 ng g^{-1} were measured in the snow samples from the
433 beginning of the sampling to the end of the second day. Later, from the beginning of the third day until

434 the end of experiment, rBC mass concentrations show an average concentration of about 5 ng g^{-1} (Figure
435 3). The average value over the whole sampling period is $9 \pm 5 \text{ ng g}^{-1}$ (approximately 6 times higher than
436 during the 85-days experiment). The rBC mass size distribution was characterized by a median value of
437 the geometric means of about $230 \pm 32 \text{ nm}$, significantly lower than that which was measured during the
438 85-days, and still in agreement with previous studies (Sinha et al., 2018; Schwarz et al., 2013). The
439 concentrations of EC and OC measured in parallel snow samples (not of the same volume) are reported
440 and described in Figure S4; the interpretation of the differences between the rBC and the EC
441 measurements in snow samples was beyond this manuscript's objectives.

442 The number concentration of coarse mode particles remains stable in the first half of the
443 experiment, until the end of April, and shows an average value over the three days of $26642 \pm 9261 \text{ \# mL}^{-1}$
444 ³. The water conductivity shows a similar behaviour, and it is characterized by an average of $39 \pm 9 \text{ \#S}$
445 (30% higher than during the 85-days experiment).

446 All the measured snow impurities show two common features (see supplementary material and
447 Figure S4): first, a decrease in the absolute values detected between 4 and 8 a.m. of April 30th, despite the
448 absence of precipitations or any other particular meteorological episode (Figure 3); second, the impact of
449 the snow precipitation event from approximately 4 p.m. to midnight of the April 30th, where the
450 concentrations of aerosols in the snow slightly increased at the very beginning whereas decreasing at the
451 end of the event. Only the BC core diameter remained above the average when the other aerosol snow
452 content decreased (up to approximately 400 nm of mass equivalent diameter), consequently returning to
453 the average value. The spatial variability of BC, calculated as proposed by Spolaor et al. (2019) for other
454 species, was obtained by the analysis of 5 surface snow samples, collected in the four corners of the
455 sampling area and one in the centre obtaining the following concentrations: a) 10.17 ng g^{-1} , b) 10.64 ng g^{-1} ,
456 c) 7.04 ng g^{-1} , d) 11.98 ng g^{-1} , and e) 11.91 ng g^{-1} , thus resulting in a spatial variability of 19%. Clear
457 sky conditions were observed for the duration of the sampling period except for the snowfall occurred at
458 the end of the third day.

459

460 3.2.2 Statistical Results

461 The multiple linear regression model for the 3-days experiment explains the 78% of the snow
462 rBC mass concentration variance, a percentage higher than the 85-days experiment, likely due to the more
463 stable atmospheric conditions and the greater interaction with the atmosphere of the upper 3 cm of the
464 snow pack compared with the depth resolution used during the seasonal experiment. Similar for the 85-
465 days experiment we evaluate (Figure S4) the 10 days back-trajectory during the 3 days of the experiment.
466 The result suggests that the air mass arriving in Ny-Ålesund during the experiment were mainly
467 originated from the Arctic Ocean.

468 The fitted multiple linear regression model indicates a statistically significant association between
469 the logarithm of the rBC mass concentration in the snow and the logarithm of the conductivity ($p <$
470 0.001), the logarithm of the number concentration of coarse-mode particles ($p < 0.001$) and the
471 occurrence of snow precipitations ($p < 0.001$). The estimated coefficients of the covariates are reported in
472 Table 1. In Figure 4 are displayed the 95% and 90% confidence intervals for the estimated coefficients of
473 regression models fitted to two experiments (85-days and the 3-days). Since the covariates considered in
474 the two experiments have quite different unit scales, Figure 4 shows the confidence intervals for the
475 standardized covariates. The standardization simplifies the comparison among the estimated effects of the
476 different covariates and between the two experiments, in this way allowing a visual comparison of the
477 estimated statistical associations between the logarithm of the snow rBC mass concentration and the
478 considered parameters.

479 The association between the logarithm of the coarse-mode particles number concentration and the
480 logarithm of the snow rBC mass concentration is positive and strongly significant ($p < 0.001$), similarly to
481 what observed for the 85-days experiment, confirming the similar behaviour of these types of particles
482 also in the surface snow pack (3 cm). The association between the logarithm of conductivity and the
483 logarithm of the snow rBC mass concentration is positive and strongly significant ($p < 0.001$). Snow
484 conductivity is mostly influenced by the presence of sea salt ions (mainly coming from sea spray aerosol
485 considering the location of the experimental site) in the snow samples. Sea spray aerosol is not considered
486 a source of rBC and a direct effect of the sea spray emission on the rBC snow concentration is here
487 consider negligible. However the positive association between rBC and conductivity can be explained by
488 the fact that both sea spray aerosol and BC particles (as well dust) undergoes to similar dry deposition
489 process (when concentration increase) favoured by the stable atmospheric condition occurred during the
490 experiment (with the exception of the snow event during the third day) as well from similar physical
491 removal process (concentration decrease) from the snow surface. Considering we are exploring the rBC
492 concentration change in the upper 3 cm, we explore the possible existence of a daily cycle. The BC
493 particles are known to be non-volatile and not photo-chemically active, therefore the decrease/increase in
494 their concentration observed during the experiment can only be driven by physical process such as wind
495 erosion and snow deposition. However an additional process that might drive the rBC concentration
496 change in the upper snow pack is the condensation of water vapour on the top of the snow crystals and the
497 formation of surface hoar as well the sublimation. The formation of surface hoar has the effect to adding
498 “water” mass without BC particles in the snow surface causing a relative rBC dilution, while sublimation
499 has the effect remove “water” mass causing a relative concentration increase. Surface hoar and
500 sublimation are depending mainly by the temperature and solar radiation, two parameters that exhibits the
501 diurnal cycle (Figure 4). From the statistical analysis no associations were found on rBC with the

502 incoming solar radiation (at hour resolution) and the snow temperature during the sampling period. These
503 results indicate that the rBC mass concentration in the surface snow does not undergo to diurnal changes
504 and this process are negligible in controlling the rBC snow surface concentration.

505 The occurrence of snow precipitations is negatively associated with the logarithm of the rBC
506 mass concentration in the snow ($p < 0.001$). As previously remarked, the aerosol scavenging intensity is
507 not measurable with snow sampling strategies based on the sampling of a constant snow thickness from
508 the surface (3 cm in this case). We tentatively explain the negative relation observed in this study with the
509 high frequency sampling, being able to follow the evolution of the BC particles scavenged during a snow
510 episode (from 3 to 12 p.m. of the 30th April 2015). The beginning of the precipitation episodes appeared
511 to remove the highest amount of BC particles, leaving the atmosphere cleaner as reflected by the lower
512 BC mass concentration revealed in subsequent samples. The snow collected at 18:00 of April 30 showed
513 a higher amount of rBC as well as the highest coarse mode particles number concentration and
514 conductivity. In the next few hours, from 9 to 12 p.m., the snow precipitations were depleted in terms of
515 aerosol content and rBC mass concentration.

516

517 **4. Conclusions and Future Perspectives**

518 The seasonal and daily experiments (85- and 3-days long, respectively) suggest that the rBC
519 concentration in the upper snow layer is not only driven by a cumulative process, as it happens when the
520 entire annual snow pack is evaluated, but it is a rather more complex process involving atmospheric,
521 meteorological and snowpack conditions. Our results based on a multiple linear regression models
522 suggest that the amount of BC in the surface snow is not associated to the BC atmospheric load. This
523 finding suggests that, despite the potentially high atmospheric BC concentrations (as in the case of long-
524 range transport of biomass burning plumes), this parameter does not seem to be the primary driver of the
525 variations in the surface snow rBC over the experiment periods. In both experiments, the coarse mode
526 particles are positively associated with the snow BC mass concentration, suggesting that the BC and
527 coarse mode particles deposition undergo similar deposition and, in case, to post-depositional processes in
528 the upper snowpack. Specifically, before the beginning of the melting season, the wet deposition episodes
529 appeared to have major impacts, whereas the activation of common local sources favour the wind
530 suspension from uncovered areas enhancing the intensity of dry deposition processes, might lead to an
531 accelerated snow melting.

532 Our results also suggest that in order to explain the observed BC mass concentration variability
533 during seasonal and diurnal time ranges other processes than wet and dry depositions should be
534 considered. Surface melting episodes enrich the BC content in the surface layer not because of an
535 enhanced deposition but mainly because of water mass loss. In particular, the snow mass loss is stronger

536 during the snow-melting season, where an increase in the rBC concentration could significantly alter the
537 snow albedo and further enhance the radiative absorption, hence promoting a positive feedback. The
538 proposed processes and the rBC concentration determined in Ny-Ålesund could be influenced by local
539 emission in particular at the beginning and at the end of the snow season when the snowpack does not cover
540 homogeneously the surface. However, the process described by our results could occur in other Arctic
541 sites although with different magnitudes and impacts.

542 The remarkable diurnal and daily variability, as well as the complex interdependent mechanisms
543 affecting the rBC mass concentration in the Arctic surface snow, makes the results of albedo-based
544 radiative impact model of the active layer a potential source of erroneous conclusions: the impacts of long
545 distance biomass burning episodes might be overestimated, whereas the impact of local sources and dry
546 deposited impurities during the melting season might be underestimated. Additional empirical studies are
547 therefore necessary in order to improve our understanding of the involved physical mechanisms and to
548 better constrain modelling studies.

549

550 **Acknowledgements**

551 This work was part of the PhD (in “Science and Management of Climate Change”) of Michele Bertò at
552 the Ca’ Foscari University of Venice that was partly funded with the Early Human Impact ERC project.
553 Thanks to Giuseppe Pellegrino for helping collecting the samples. Thanks to Jacopo Gabrieli and the
554 technicians of the Ca’ Foscari University of Venice for the precious help in building up the coarse mode
555 particles and conductivity measurement apparatus. We acknowledge the use of data and imagery from
556 LANCE FIRMS operated by the NASA/GSFC/Earth Science Data and Information System (ESDIS) with
557 funding provided by NASA/HQ. We want to thank Paolo Laj and the LGGE (Grenoble, France) for
558 lending us the SP2 and Marco Zanatta for transferring the SP2 know-how on instrumental functioning and
559 data analyses. Thanks to Martin Gysel-Beer, PSI, for the IGOR based SP2 Toolkit for SP2 data analyses.
560 We thank Marion Maturilli and AWI for providing us with the meteorological data. Thanks to Giorgio
561 Bertò for checking and correcting the language of this manuscript. This paper is an output of the AMIS
562 project in the framework of “Project MIUR – Dipartimenti di Eccellenza 2018-2022”. This project has
563 received funding from the European Union's Horizon 2020 research and innovation programme under
564 grant agreement No 689443 via project iCUPE (Integrative and Comprehensive Understanding on Polar
565 Environments).

566

567

568

569 **Data Availability**

570 Meteorological and surface radiation data are available at the PANGAEA database (Maturilli, 2015a;
571 2015b; 2015c; 2016a; 2016b; 2018a; 2018b; 2018c; 2018d; 2018e). The data for precipitation amount at
572 Ny-Ålesund can be accessed via the eKlima database of MET Norway. The BC data are available upon
573 request.

574

575 **Author Contributions**

576 Author contributions. AS, EB, DC and MB conceived the experiments; AS, EB, DC, and LP collected the
577 samples; MB measured the samples; KM and MMaz provided the atmospheric eBC concentrations; SC
578 and DC provided the back-trajectories analyses; CV performed the statistical analyses with inputs from
579 MB and AS. MB prepared the manuscript mainly with inputs from AS, J-C. G and DC (in the methods
580 section from AS, KM, MMaz) and all co-authors contributed to the interpretation of the results as well as
581 manuscript review and editing.

582

583 **Data repository**

584 Maturilli, Marion (2020): Basic and other measurements of radiation and continuous meteorological
585 observations at station Ny-Ålesund (April, May 2014 and April, May, June 2015), reference list of 10
586 datasets. Alfred Wegener Institute - Research Unit Potsdam, PANGAEA,
587 <https://doi.pangaea.de/10.1594/PANGAEA.913988> (DOI registration in progress)

588

589 **Competing interests**

590 The authors declare that they have no conflict of interest.

591

592

593

594

595

596

597

598

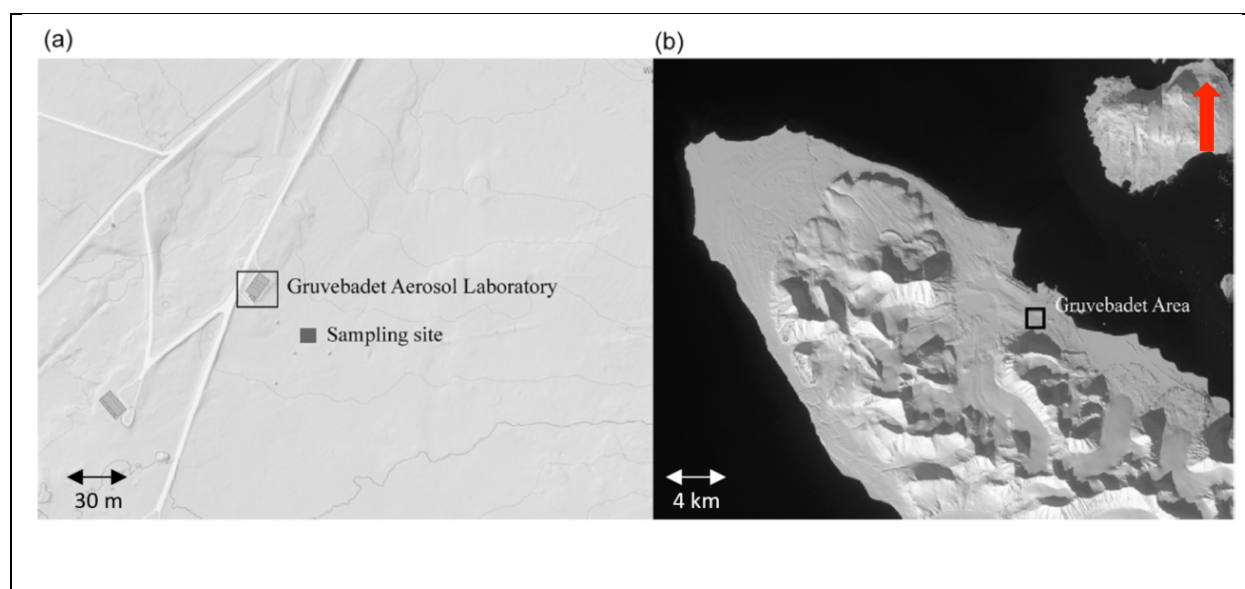
599

600

601 **FIGURES**

602 **Figure 1.** a) Experimental sampling site location (dark grey rectangle), in proximity of the Gruvebadet
603 Aerosol Laboratory. b) Gruvebadet area (black square), close to the Ny-Ålesund research village. From:
604 Spolaor et al., 2019 (maps from <https://toposvalbard.npolar.no/>). The red arrow points to the North.

605



606

607

608

609

610

611

612

613

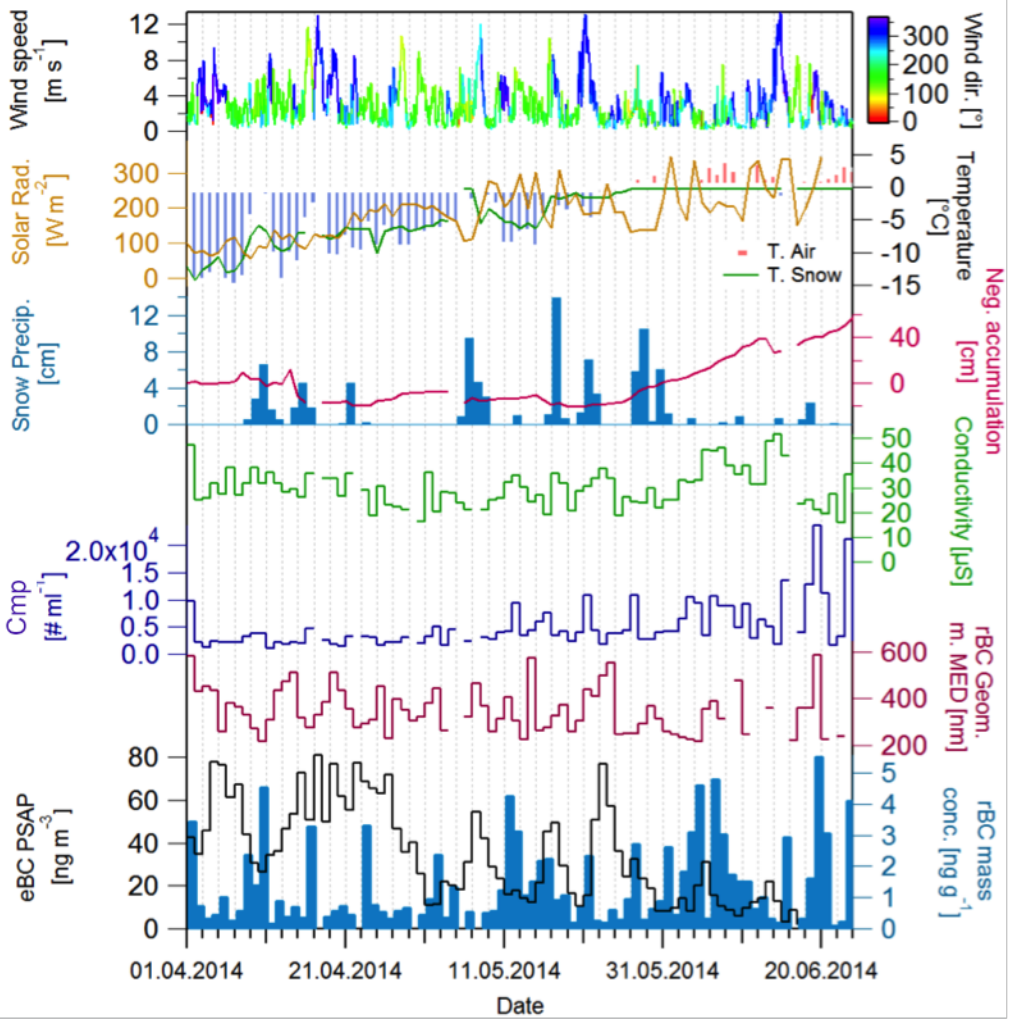
614

615

616

617 **Figure 2.** The 85-days experiments daily snow samples rBC mass concentration (light blue), eBC mass
618 concentration in the atmosphere (black), geometric mean mass equivalent diameter (purple), number of
619 coarse mode particles (Cmp - blue), total conductivity (green), meteo/snow parameters used in the
620 statistical exercise: wind speed color coded for wind direction, solar radiation (orange line), air and
621 surface snow temperatures (blue bars and green line respectively), amount of fresh snow (“snow
622 precipitations”, light blue bars) and the snow accumulation (“Neg. accumulation”; the values were
623 multiplied by -1 in order to show the similar trend of the snow lost and of the air/snow temperature during
624 the melting period at the end of the campaign).

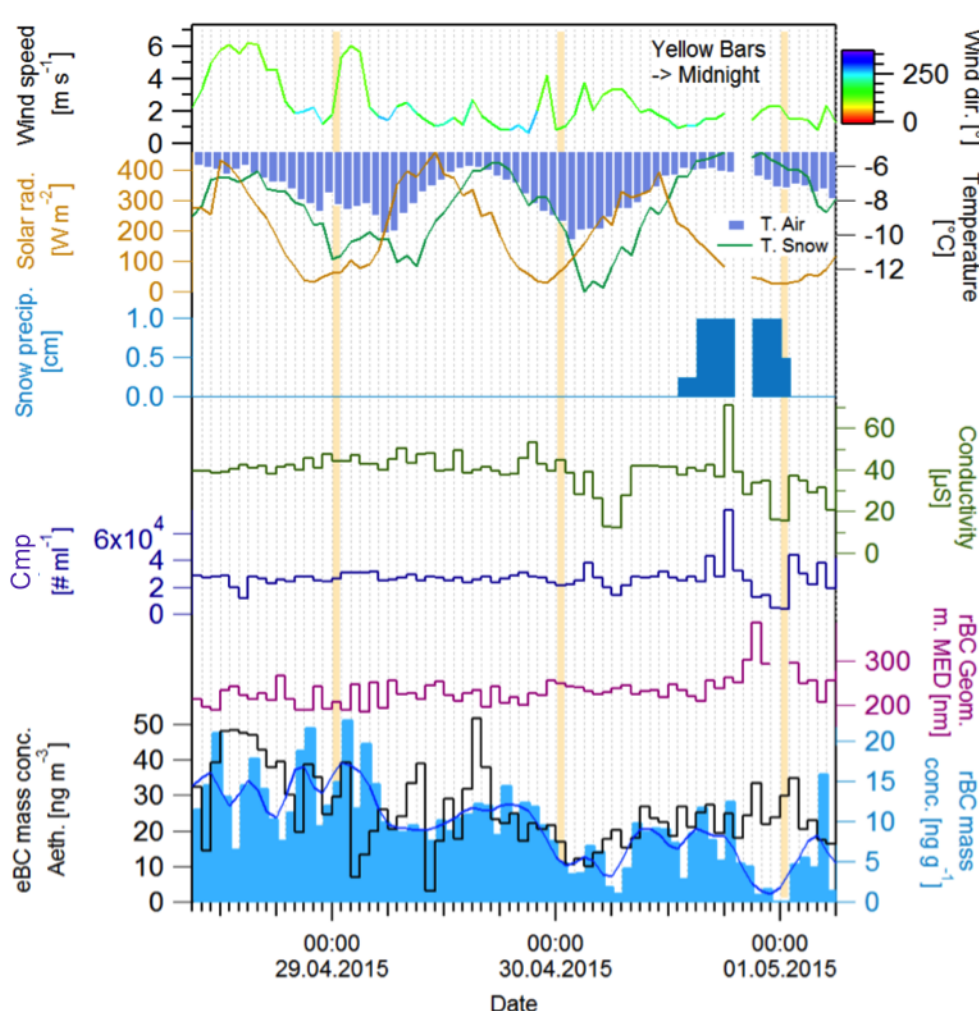
625



626

627

628 **Figure 3.** The 3-days experiments snow samples hourly rBC mass concentration and smoothed line (light
 629 blue bars), atmospheric eBC mass concentration in the atmosphere (black), geometric mean mass
 630 equivalent diameter (purple), the number concentration of coarse mode particles (Cmp - blue) and the
 631 total conductivity (green), meteo/snow parameters used in the statistical exercise: wind speed color coded
 632 for wind direction, solar radiation (Orange line), Air and surface snow temperature (blue bars and green
 633 line respectively), amount of fresh snow (“snow precipitations”, light blue bars). The yellow bars are
 634 centered on the midnight hours for the three sampling days.



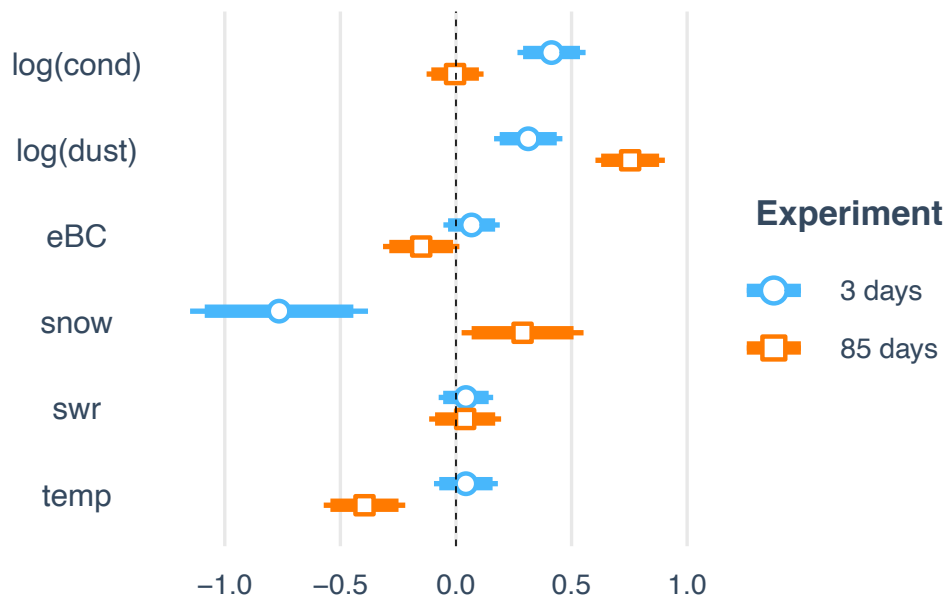
636

637

638 **Figure 4.** Estimated coefficients of the standardized covariates of the multiple linear regression models
 639 fitted to the 3 days and 85 days experiments. The segments correspond to 95% confidence intervals about
 640 the corresponding estimated coefficients. The internal thicker segments correspond to 90% confidence
 641 intervals. Intervals, that do not include the zero, correspond to statistically significant covariates. If a
 642 confidence interval consists of positive values, then there is a significant positive association between the
 643 corresponding covariate and the logarithm of the snow rBC mass concentration **conditionally to**
 644 **the remaining covariates**. Vice versa, if the confidence interval consists of negative values, then the
 645 association is negative. The abbreviations used in the plot are: “log(cond)” – logarithm of the water
 646 conductivity time series, “log(dust)” – logarithm of the coarse mode particles number concentration time
 647 series, “eBC” – equivalent black carbon atmospheric concentration, “snow” – presence of snow

648 precipitation episodes, “swr” – short wave radiation, “temp” – the snow temperature. The plot is produced
649 with the R package (R Core Team, 2020) jtools (Long, 2020).

650



651

652

653

654

655 **TABLES**

656

657 **Table 1.** Estimated coefficients, 95% confidence intervals and the corresponding p-values for the
 658 covariates of the multiple linear regression model fitted to the 85 days and the 3-days experiments. The
 659 last rows of the table report the number of observations, the multiple coefficient of determination (R^2) and
 660 its adjusted version.

661

<i>Covariates</i>	85-days			3-days		
	<i>Estimates</i>	<i>CI</i>	<i>p</i>	<i>Estimates</i>	<i>CI</i>	<i>p</i>
Intercept	-6.74	-8.74 – -4.74	< 0.001	1.39	-2.30 – 5.09	0.453
Cond[log]	-0.02	-0.51 – 0.48	0.950	1.38	0.89 – 1.87	< 0.001
Dust[log]	1.29	1.03 – 1.55	< 0.001	0.74	0.39 – 1.09	< 0.001
eBC	-0.01	-0.01 – 0.00	0.074	0.00	-0.00 – 0.01	0.272
Snow[TRUE]	0.29	0.02 – 0.55	0.033	-0.77	-1.15 – -0.38	< 0.001
SWR	0.00	-0.00 – 0.00	0.613	0.00	-0.00 – 0.00	0.468
Temp	-0.10	-0.14 – -0.05	< 0.001	0.02	-0.04 – 0.08	0.535
Observation	72			68		
R2 /R2 adjusted	0.688/0.6590			0.779 /0.758		

662

663

664

665

666

667

668

669

670

671

672 **References**

673 Aamaas, B., Bøggild, C. E., Stordal, F., Berntsen, T., Holmèn, K. and Strøm, J.: Elemental carbon
674 deposition to Svalbard snow from Norwegian settlements and long-range transport, *Tellus B Chem.*
675 *Phys. Meteorol.*, 63(3), 340–351, doi:10.1111/j.1600-0889.2011.00531.x, 2011.

676 AMAP, A. M. and A.: ARCTIC MONITORING AND ASSESSMENT PROGRAMME (AMAP): Work
677 Plan 2015–2017., Working Paper, Arctic Monitoring and Assessment Programme (AMAP). [online]
678 Available from: <https://oarchive.arctic-council.org/handle/11374/1443> (Accessed 6 May 2020), 2015.

679 Andreae, M. O. and Merlet, P.: Emission of trace gases and aerosols from biomass burning, *Glob.*
680 *Biogeochem. Cycles*, 15(4), 955–966, doi:10.1029/2000GB001382, 2001.

681 Bazzano, A., Ardini, F., Becagli, S., Traversi, R., Udisti, R., Cappelletti, D. and Grotti, M.: Source
682 assessment of atmospheric lead measured at Ny-Ålesund, Svalbard, *Atmos. Environ.*, 113, 20–26,
683 doi:10.1016/j.atmosenv.2015.04.053, 2015.

684 Bond, T. C., Anderson, T. L. and Campbell, D.: Calibration and Intercomparison of Filter-Based
685 Measurements of Visible Light Absorption by Aerosols, *Aerosol Sci. Technol.*, 30(6), 582–600,
686 doi:10.1080/027868299304435, 1999.

687 Bond, T. C., Doherty, S. J., Fahey, D. W., Forster, P. M., Berntsen, T., DeAngelo, B. J., Flanner, M. G.,
688 Ghan, S., Kärcher, B., Koch, D., Kinne, S., Kondo, Y., Quinn, P. K., Sarofim, M. C., Schultz, M. G.,
689 Schulz, M., Venkataraman, C., Zhang, H., Zhang, S., Bellouin, N., Guttikunda, S. K., Hopke, P. K.,
690 Jacobson, M. Z., Kaiser, J. W., Klimont, Z., Lohmann, U., Schwarz, J. P., Shindell, D., Storelvmo, T.,
691 Warren, S. G. and Zender, C. S.: Bounding the role of black carbon in the climate system: A scientific
692 assessment: BLACK CARBON IN THE CLIMATE SYSTEM, *J. Geophys. Res. Atmospheres*, 118(11),
693 5380–5552, doi:10.1002/jgrd.50171, 2013.

694 Cohen, J., Screen, J. A., Furtado, J. C., Barlow, M., Whittleston, D., Coumou, D., Francis, J., Dethloff,
695 K., Entekhabi, D., Overland, J. and Jones, J.: Recent Arctic amplification and extreme mid-latitude
696 weather, *Nat. Geosci.*, 7(9), 627–637, doi:10.1038/ngeo2234, 2014.

697 Comiso, J. C., Parkinson, C. L., Gersten, R. and Stock, L.: Accelerated decline in the Arctic sea ice cover,
698 *Geophys. Res. Lett.*, 35(1), doi:10.1029/2007GL031972, 2008.

699 DeMott, P.J., Hill, T.C., McCluskey, C.S., Prather, K.A., Collins, D.B., Sullivan, R.C., Ruppel, M.J.,
700 Mason, R.H., Irish, V.E., Lee, T. and Hwang, C.Y.: Sea spray aerosol as a unique source of ice
701 nucleating particles. *Proceedings of the National Academy of Sciences*, 113(21), pp.5797-5803, doi:
702 10.1073/pnas.1514034112, 2016.

703 Doherty, S. J., S. G. Warren, T. C. Grenfell, A. D. Clarke, and R. E. Brandt.: Light-absorbing impurities
704 in Arctic snow. *Atmospheric Chem. Phys.*10, no. 23: 11647, doi: 10.5194/acp-10-11647-2010, 2010.

705 Doherty, S. J., T. C. Grenfell, S. Forsström, D. L. Hegg, S. G. Warren and R. Brandt, Observed vertical
706 redistribution of black carbon and other light-absorbing particles in melting snow, *J. Geophys. Res.*,
707 118(11), 5553-5569, doi:10.1002/jgrd.50235, 2013.

708 Doherty, S. J., D. A. Hegg, P. K. Quinn, J. E. Johnson, J. P. Schwarz, C. Dang and S. G. Warren, Causes
709 of variability in light absorption by particles in snow at sites in Idaho and Utah, *J. Geophys. Res. -*
710 *Atmos.*, 121, doi:10.1002/2015JD024375, 2016.

- 711 Eckhardt, S., Hermansen, O., Grythe, H., Fiebig, M., Stebel, K., Cassiani, M., Baecklund, A. and Stohl,
712 A.: The influence of cruise ship emissions on air pollution in Svalbard - a harbinger of a more polluted
713 Arctic?, *Atmospheric Chem. Phys.*, 13(16), 8401–8409, doi: 10.5194/acp-13-8401-2013, 2013.
- 714 Eckhardt, S., Quennehen, B., Olivieri, D. J. L., Berntsen, T. K., Cherian, R., Christensen, J. H., W. Collins
715 et al.: Current model capabilities for simulating black carbon and sulfate concentrations in the Arctic
716 atmosphere: a multi-model evaluation using a comprehensive measurement data set. *Atmospheric*
717 *Chem. Phys.*, 15, no. 16: 9413-9433, doi: 10.5194/acp-15-9413-2015, 2015.
- 718 Eleftheriadis, K., Vratolis, S. and Nyeki, S.: Aerosol black carbon in the European Arctic: Measurements
719 at Zeppelin station, Ny-Ålesund, Svalbard from 1998–2007, *Geophys. Res. Lett.*, 36(2),
720 doi:10.1029/2008GL035741, 2009.
- 721 Feltracco, M., Barbaro, E., Kirchgeorg, T., Spolaor, A., Turetta, C., Zangrando, R., Barbante, C. and
722 Gambaro, A.: Free and combined L- and D-amino acids in Arctic aerosol, *Chemosphere*, 220, 412–421,
723 doi:10.1016/j.chemosphere.2018.12.147, 2019.
- 724 Feltracco, M., Barbaro, E., Tedeschi, S., Spolaor, A., Turetta, C., Vecchiato, M., Morabito, E.,
725 Zangrando, R., Barbante, C. and Gambaro, A.: Interannual variability of sugars in Arctic aerosol:
726 Biomass burning and biogenic inputs, *Sci. Total Environ.*, 706, 136089,
727 doi:10.1016/j.scitotenv.2019.136089, 2020.
- 728 Feltracco, M., Barbaro, E., Spolaor, A., Vecchiato, M., Callegaro, A., Burgay, F., Vardè, M., Maffezzoli,
729 N., Dallo, F., Scoto, F., Zangrando, R., Barbante, C., Gambaro, A.: Year-round measurements of size-
730 segregated low molecular weight organic acids in Arctic aerosol. *Sci. Total Environ.*, 763, 142954, doi:
731 10.1016/j.scitotenv.2020.142954, 2021a.
- 732 Feltracco, M., Barbaro, E., Hoppe, C. J., Wolf, K. K., Spolaor, A., Layton, R., Keuschnig, C., Barbante,
733 C., Gambaro, A., Larose, C.: Airborne bacteria and particulate chemistry capture Phytoplankton bloom
734 dynamics in an Arctic fjord, *Atmos. Environ.*, 256, 118458, doi: 10.1016/j.atmosenv.2021.118458,
735 2021b.
- 736 Ferrero, L., Cappelletti, D., Busetto, M., Mazzola, M., Lupi, A., Lanconelli, C., Becagli, S., Traversi, R.,
737 Caiazzo, L., Giardi, F., Moroni, B., Crocchianti, S., Fierz, M., Mocnik, G., Sangiorgi, G., Perrone, M.
738 G., Maturilli, M., Vitale, V., Udisti, R. and Bolzacchini, E.: Vertical profiles of aerosol and black carbon
739 in the Arctic: a seasonal phenomenology along two years (2011-2012) of field campaign, *Atmospheric*
740 *Chem. Phys.*, 16, 12601–12629, doi: 10.5194/acp-16-12601-2016, hdl:10013/epic.48736, 2016.
- 741 Flanner, M. G.: Arctic climate sensitivity to local black carbon, *J. Geophys. Res. Atmospheres*, 118(4),
742 1840–1851, doi:10.1002/jgrd.50176, 2013.
- 743 Flanner, M. G., Zender, C. S., Randerson, J. T. and Rasch, P. J.: Present-day climate forcing and response
744 from black carbon in snow, *J. Geophys. Res. Atmospheres*, 112(D11), doi:10.1029/2006JD008003,
745 2007.
- 746 Forsström, S., Ström, J., Pedersen, C. A., Isaksson, E. and Gerland, S.: Elemental carbon distribution in
747 Svalbard snow, *J. Geophys. Res. Atmospheres*, 114(D19), doi:10.1029/2008JD011480, 2009.
- 748 Forsström, S., Isaksson, E., Skeie, R. B., Ström, J., Pedersen, C. A., Hudson, S. R., Berntsen, T. K.,
749 Lihavainen, H., Godtliebsen, F. and Gerland, S.: Elemental carbon measurements in European Arctic
750 snowpacks, *J. Geophys. Res. Atmospheres*, 118(24), 13,614-13,627, doi:10.1002/2013JD019886, 2013.

751 Gallet JC, Björkman M, Larose C, Luks B., Martma T. and Zdanowics C. (eds). Protocols and
752 recommendations for the measurement of snow physical properties, and sampling of snow for black
753 carbon, water isotopes, major ions and micro-organisms. Norwegian Polar Institute. Kortrapport / Brief
754 Report no. 046, ISBN 978-82-7666-415-7 (printed), www.npolar.no, 2018.

755 Gogoi, M. M., Babu, S. S., Moorthy, K. K., Thakur, R. C., Chaubey, J. P. and Nair, V. S.: Aerosol black
756 carbon over Svalbard regions of Arctic, *Polar Sci.*, 10(1), 60–70, doi:10.1016/j.polar.2015.11.001, 2016.

757 Gundel, L. A., Dod, R. L., Rosen, H. and Novakov, T.: Relationship between optical attenuation and
758 black carbon concentration for ambient and source particles, Lawrence Berkeley Lab., CA (USA).
759 [online] Available from: <https://www.osti.gov/biblio/5653266> (Accessed 7 May 2020), 1983.

760 Hadley, O. L. and Kirchstetter, T. W.: Black-carbon reduction of snow albedo, *Nat. Clim. Change*, 2(6),
761 437–440, doi:10.1038/nclimate1433, 2012.

762 Hansen, J. and Nazarenko, L.: Soot climate forcing via snow and ice albedos, *Proc. Natl. Acad. Sci.*,
763 101(2), 423–428, doi:10.1073/pnas.2237157100, 2004.

764 Ingersoll, G.P., Don Campbell, M. Alisa Mast, David W. Clow, Leora Nanus, and Brent Frakes. 2009.
765 Snowpack Chemistry Monitoring Protocol for the Rocky Mountain Network; Narrative and Standard
766 Operating Procedures. United States Geological Service (USGS), Reston, Virginia. Administrative
767 Report, 2009

768 Jacobi, H.-W., Obleitner, F., Da Costa, S., Ginot, P., Eleftheriadis, K., Aas, W. and Zanatta, M.:
769 Deposition of ionic species and black carbon to the Arctic snowpack: combining snow pit observations
770 with modeling, 10361-10377, doi:10.5194/acp-19-10361-2019, 2019.

771 Khan, A. L., Dierssen, H., Schwarz, J. P., Schmitt, C., Chlus, A., Hermanson, M., Painter, T. H. and
772 McKnight, D. M.: Impacts of coal coarse mode from an active mine on the spectral reflectance of
773 Arctic surface snow in Svalbard, Norway, *J. Geophys. Res. Atmospheres*, 122(3), 1767–1778,
774 doi:10.1002/2016JD025757, 2017.

775 Laborde, M., Crippa, M., Tritscher, T., Jurányi, Z., Decarlo, P. F., Temime-Roussel, B., Marchand, N.,
776 Eckhardt, S., Stohl, A., Baltensperger, U., Prévôt, A. S. H., Weingartner, E. and Gysel, M.: Black
777 carbon physical properties and mixing state in the European megacity Paris, *Atmospheric Chem. Phys.*,
778 13(11), 5831–5856, doi:10.5194/acp-13-5831-2013, 2013.

779 Laj, P., Bigi, A., Rose, C., Andrews, E., Lund Myhre, C., Collaud Coen, M., Wiedensohler, A., Schultz,
780 M., Ogren, J. A., Fiebig, M., Gliß, J., Mortier, A., Pandolfi, M., Petäjä, T., Kim, S.-W., Aas, W., Putaud,
781 J.-P., Mayol-Bracero, O., Keywood, M., Labrador, L., Aalto, P., Ahlberg, E., Alados Arboledas, L.,
782 Alastuey, A., Andrade, M., Artíñano, B., Ausmeel, S., Arsov, T., Asmi, E., Backman, J., Baltensperger,
783 U., Bastian, S., Bath, O., Beukes, J. P., Brem, B. T., Bukowiecki, N., Conil, S., Couret, C., Day, D.,
784 Dayantolis, W., Degorska, A., Santos, S. M. D., Eleftheriadis, K., Fetfatzis, P., Favez, O., Flentje, H.,
785 Gini, M. I., Gregorič, A., Gysel-Beer, M., Hallar, G. A., Hand, J., Hoffer, A., Hueglin, C., Hooda, R. K.,
786 Hyvärinen, A., Kalapov, I., Kalivitis, N., Kasper-Giebl, A., Kim, J. E., Kouvarakis, G., Kranjc, I.,
787 Krejci, R., Kulmala, M., Labuschagne, C., Lee, H.-J., Lihavainen, H., Lin, N.-H., Lösschau, G., Luoma,
788 K., Marinoni, A., Meinhardt, F., Merkel, M., Metzger, J.-M., Mihalopoulos, N., Nguyen, N. A.,
789 Ondracek, J., Pérez, N., Perrone, M. R., Petit, J.-E., Picard, D., Pichon, J.-M., Pont, V., Prats, N., Prenni,
790 A., Reisen, F., Romano, S., Sellegri, K., Sharma, S., Schauer, G., Sheridan, P., Sherman, J. P., Schütze,
791 M., Schwerin, A., Sohmer, R., Sorribas, M., Steinbacher, M., Sun, J., Titos, G., Tokzko, B., et al.: A

792 global analysis of climate-relevant aerosol properties retrieved from the network of GAW near-surface
793 observatories, *Atmospheric Meas. Tech. Discuss.*, 1–70, doi: 10.5194/amt-2019-499, 2020.

794 Law, K. S. and Stohl, A.: Arctic Air Pollution: Origins and Impacts, *Science*, 315(5818), 1537–1540,
795 doi:10.1126/science.1137695, 2007.

796 Lim, S., Fain, X., Zanatta, M., Cozic, J., Jaffrezo, J. L., Ginot, P. and Laj, P.: Refractory black carbon
797 mass concentrations in snow and ice: method evaluation and inter-comparison with elemental carbon
798 measurement, *Atmospheric Meas. Tech.*, 7(10), 3307–3324, doi:10.5194/amt-7-3307-2014, 2014.

799 Liu, J., Fan, S., Horowitz, L. W. and Levy, H.: Evaluation of factors controlling long-range transport of
800 black carbon to the Arctic, *J. Geophys. Res. Atmospheres*, 116(D4), doi:10.1029/2010JD015145, 2011.

801 Long J.A.. *jtools: Analysis and Presentation of Social Scientific Data* (2020). URL: [https://cran.r-](https://cran.r-project.org/package=jtools)
802 [project.org/package=jtools](https://cran.r-project.org/package=jtools)

803 Lupi, A., Busetto, M., Becagli, S., Giardi, F., Lanconelli, C., Mazzola, M., Udisti, R., Hansson, H.-C.,
804 Henning, T., Petkov, B., Ström, J., Krejci, R., Tunved, P., Viola, A. P. and Vitale, V.: Multi-seasonal
805 ultrafine aerosol particle number concentration measurements at the Gruvebadet observatory, Ny-
806 Ålesund, Svalbard Islands, *Rendiconti Lincei*, 27(1), 59–71, doi:10.1007/s12210-016-0532-8, 2016.

807 Maturilli, M., Herber, A. and König-Langlo, G.: Climatology and Time Series of Surface Meteorology in
808 Ny-Ålesund, Svalbard, *Earth Syst. Sci. Data*, 5, 155–163, doi: 10.5194/essd-5-155-2013, 2013.

809 Maturilli, M., Herber, A. and König-Langlo, G.: Surface radiation climatology for Ny-Ålesund, Svalbard
810 (78.9° N), basic observations for trend detection, *Theor. Appl. Climatol.*, 120(1), 331–339,
811 doi:10.1007/s00704-014-1173-4, 2015.

812 Maturilli, M., Hanssen-Bauer, I., Neuber, R., Rex, M. and Edvardsen, K.: The Atmosphere Above Ny-
813 Ålesund: Climate and Global Warming, Ozone and Surface UV Radiation, in *The Ecosystem of*
814 *Kongsfjorden, Svalbard*, edited by H. Hop and C. Wiencke, pp. 23–46, Springer International
815 Publishing, Cham., 2019.

816 Meinander, O.; Heikkinen, E.; Aurela, M.; Hyvärinen, A. Sampling, Filtering, and Analysis Protocols to
817 Detect Black Carbon, Organic Carbon, and Total Carbon in Seasonal Surface Snow in an Urban
818 Background and Arctic Finland (>60° N). *Atmosphere* 2020, 11, 923.
819 <https://doi.org/10.3390/atmos11090923>, 2020a.

820 Moosmüller, H., Chakrabarty, R. K. and Arnott, W. P.: Aerosol light absorption and its measurement: A
821 review, *J. Quant. Spectrosc. Radiat. Transf.*, 110(11), 844–878, doi:10.1016/j.jqsrt.2009.02.035, 2009.

822 Mori, T., Goto-Azuma, K., Kondo, Y., Ogawa-Tsukagawa, Y., Miura, K., Hirabayashi, M., Oshima, N.,
823 Koike, M., Kupiainen, K., Moteki, N., Ohata, S., Sinha, P. R., Sugiura, K., Aoki, T., Schneebeli, M.,
824 Steffen, K., Sato, A., Tsushima, A., Makarov, V., Omiya, S., Sugimoto, A., Takano, S. and Nagatsuka,
825 N.: Black Carbon and Inorganic Aerosols in Arctic Snowpack, *J. Geophys. Res. Atmospheres*, 124(23),
826 13325–13356, doi:10.1029/2019JD030623, 2019.

827 Moroni, B., Becagli, S., Bolzacchini, E., Busetto, M., Cappelletti, D., Crocchianti, S., Ferrero, L., Frosini,
828 D., Lanconelli, C., Lupi, A., Maturilli, M., Mazzola, M., Perrone, M. G., Sangiorgi, G., Traversi, R.,
829 Udisti, R., Viola, A. and Vitale, V.: Vertical Profiles and Chemical Properties of Aerosol Particles upon
830 Ny-Ålesund (Svalbard Islands), *Adv. Meteorol.*, 2015, e292081, doi: 10.1155/2015/292081, 2015.

831 Moroni, B., Arnalds, O., Dagsson-Waldhauserová, P., Crocchianti, S., Vivani, R. and Cappelletti, D.:
832 Mineralogical and Chemical Records of Icelandic Coarse mode Sources Upon Ny-Ålesund (Svalbard
833 Islands), *Front. Earth Sci.*, 6, doi:10.3389/feart.2018.00187, 2018.

834 Moroni, B., Ritter, C., Crocchianti, S., Markowicz, K., Mazzola, M., Becagli, S., et al.. Individual particle
835 characteristics, optical properties and evolution of an extreme long-range transported biomass burning
836 event in the European Arctic (Ny-Ålesund, Svalbard Islands). *Journal of Geophysical Research:*
837 *Atmospheres*, 125, e2019JD031535, doi:10.1029/2019JD031535, 2020.
838

839 Motos, G., Schmale, J., Corbin, J. C., Modini, R. L., Karlen, N., Bertò, M., Baltensperger, U. and Gysel-
840 Beer, M.: Cloud droplet activation properties and scavenged fraction of black carbon in liquid-phase
841 clouds at the high-alpine research station Jungfraujoch (3580 m a.s.l.), *Atmospheric Chem. Phys.*, 19(6),
842 3833–3855, doi:10.5194/acp-19-3833-2019, 2019.

843 Osmont, D., Wendl, I. A., Schmidely, L., Sigl, M., Vega, C. P., Isaksson, E. and Schwikowski, M.: An
844 800-year high-resolution black carbon ice core record from Lomonosovfonna, Svalbard, *Atmospheric*
845 *Chem. Phys.*, 18(17), 12777–12795, doi: 10.5194/acp-18-12777-2018, 2018.

846 Pedersen, C. A., Gallet, J.-C., Ström, J., Gerland, S., Hudson, S. R., Forsström, S., Isaksson, E. and
847 Berntsen, T. K.: In situ observations of black carbon in snow and the corresponding spectral surface
848 albedo reduction, *J. Geophys. Res. Atmospheres*, 120(4), 1476–1489, doi: 10.1002/2014JD022407,
849 2015.

850 Perovich, D. : Light reflection and transmission by a temperate snow cover. *Journal of Glaciology*,
851 53(181), 201-210. doi:10.3189/172756507782202919, 2007
852

853 Petzold, A., Ogren, J. A., Fiebig, M., Laj, P., Li, S.-M., Baltensperger, U., Holzer-Popp, T., Kinne, S.,
854 Pappalardo, G., Sugimoto, N., Wehrli, C., Wiedensohler, A. and Zhang, X.-Y.: Recommendations for
855 reporting “black carbon” measurements, *Atmospheric Chem. Phys.*, 13(16), 8365–8379, doi:
856 10.5194/acp-13-8365-2013, 2013.

857 R Core Team. R: A language and environment for statistical computing. R Foundation for Statistical
858 Computing, Vienna, Austria, (2020). URL: <https://www.R-project.org/>

859 Ruppel, M. M., Soares, J., Gallet, J.-C., Isaksson, E., Martma, T., Svensson, J., Kohler, J., Pedersen, C.
860 A., Manninen, S., Korhola, A. and Ström, J.: Do contemporary (1980–2015) emissions determine the
861 elemental carbon deposition trend at Holtedahlfonna glacier, Svalbard?, *Atmospheric Chem. Phys.*,
862 17(20), 12779–12795, doi: 10.5194/acp-17-12779-2017, 2017.

863 Scalabrin, E., Zangrando, R., Barbaro, E., Kehrwald, N. M., Gabrieli, J., Barbante, C. and Gambaro, A.:
864 Amino acids in Arctic aerosols, *Atmospheric Chem. Phys.*, 12(21), 10453–10463, doi:10.5194/acp-12-
865 10453-2012, 2012.

866 Schmale, J., Arnold, S. R., Law, K. S., Thorp, T., Anenberg, S., Simpson, W. R., Mao, J. and Pratt, K. A.:
867 Local Arctic Air Pollution: A Neglected but Serious Problem, *Earths Future*, 6(10), 1385–1412,
868 doi:10.1029/2018EF000952, 2018.

869 Schwarz, J. P., Gao, R. S., Perring, A. E., Spackman, J. R. and Fahey, D. W.: Black carbon aerosol size in
870 snow, *Sci. Rep.*, 3(1), 1–5, doi:10.1038/srep01356, 2013.

- 871 Screen, J. A. and Simmonds, I.: The central role of diminishing sea ice in recent Arctic temperature
872 amplification, *Nature*, 464(7293), 1334–1337, doi:10.1038/nature09051, 2010.
- 873 Segura, S., Estellés, V., Titos Vela, G., Lyamani, H., Utrilla Navarro, P., Zotter, P., Prévot, A. S. H.,
874 Močnik, G., Alados-Arboledas, L. and Martínez-Lozano, J. A.: Determination and analysis of in situ
875 spectral aerosol optical properties by a multi-instrumental approach, doi:10.5194/amt-7-2373-2014,
876 2014.
- 877 Serreze, M. C. and Barry, R. G.: Processes and impacts of Arctic amplification: A research synthesis,
878 *Glob. Planet. Change*, 77(1), 85–96, doi:10.1016/j.gloplacha.2011.03.004, 2011.
- 879 Sharma, S., W. Richard Leaitch, Lin Huang, Daniel Veber, Felicia Kolonjari, Wendy Zhang. An
880 evaluation of three methods for measuring black carbon in Alert, Canada. *Atmos. Chem. Phys.*, 17,
881 15225-15243, <https://doi.org/10.5194/acp-17-15225-2017>, 2017.
- 882 Sinha, P. R., Y. Kondo, M. Koike, J. Ogren, A. Jefferson, T. Barrett, R. Sheesley, S. Ohata, N. Moteki, H.
883 Coe, D. Liu, M. Irwin, P. Tunved, P. K. Quinn, and Y. Zhao, Evaluation of ground-based black carbon
884 measurements by filter-based photometers at two Arctic sites, *J. Geophys. Res.*, 122,
885 doi:10.1002/2016JJD025843, 2017.
- 886 Sinha, P. R., Kondo, Y., Goto-Azuma, K., Tsukagawa, Y., Fukuda, K., Koike, M., Ohata, S., Moteki, N.,
887 Mori, T., Oshima, N., Førland, E. J., Irwin, M., Gallet, J.-C. and Pedersen, C. A.: Seasonal Progression
888 of the Deposition of Black Carbon by Snowfall at Ny-Ålesund, Spitsbergen: Deposition of Black
889 Carbon in Spitsbergen, *J. Geophys. Res. Atmospheres*, 123(2), 997–1016, doi:10.1002/2017JD028027,
890 2018.
- 891 Skiles, S. M. and Painter, T. H.: Toward Understanding Direct Absorption and Grain Size Feedbacks by
892 Coarse mode Radiative Forcing in Snow With Coupled Snow Physical and Radiative Transfer
893 Modeling, *Water Resour. Res.*, 55(8), 7362–7378, doi:10.1029/2018WR024573, 2019.
- 894 Skiles, S. M., Flanner, M., Cook, J. M., Dumont, M. and Painter, T. H.: Radiative forcing by light-
895 absorbing particles in snow, *Nat. Clim. Change*, 8(11), 964–971, doi:10.1038/s41558-018-0296-5, 2018.
- 896 Spolaor, A., Angot, H., Roman, M., Dommergue, A., Scarchilli, C., Vardè, M., Del Guasta, M., Pedeli,
897 X., Varin, C., Sprovieri, F., Magand, O., Legrand, M., Barbante, C. and Cairns, W. R. L.: Feedback
898 mechanisms between snow and atmospheric mercury: Results and observations from field campaigns on
899 the Antarctic plateau, *Chemosphere*, 197, 306–317, doi:10.1016/j.chemosphere.2017.12.180, 2018.
- 900 Spolaor, A., Barbaro, E., Cappelletti, D., Turetta, C., Mazzola, M., Giardi, F., Björkman, M. P.,
901 Lucchetta, F., Dallo, F., Pfaffhuber, K. A., Angot, H., Dommergue, A., Maturilli, M., Saiz-Lopez, A.,
902 Barbante, C. and Cairns, W. R. L.: Diurnal cycle of iodine, bromine, and mercury concentrations in
903 Svalbard surface snow, *Atmospheric Chem. Phys.*, 19(20), 13325–13339, doi: 10.5194/acp-19-13325-
904 2019, 2019.
- 905 Stephens, M., Turner, N. and Sandberg, J.: Particle identification by laser-induced incandescence in a
906 solid-state laser cavity, *Appl. Opt.*, 42(19), 3726–3736, doi:10.1364/AO.42.003726, 2003.
- 907 Stohl, A., Klimont, Z., Eckhardt, S., Kupiainen, K., Shevchenko, V. P., Kopeikin, V. M., and Novigatsky,
908 A. N.: Black carbon in the Arctic: the underestimated role of gas flaring and residential combustion
909 emissions., *Atmospheric Chem. Phys.*, 13(17), 8833-8855, doi: 10.5194/acp-13-8833-2013, 2013.

- 910 Tunved, P., Ström, J. and Krejci, R.: Arctic aerosol life cycle: linking aerosol size distributions observed
911 between 2000 and 2010 with air mass transport and precipitation at Zeppelin station, Ny-Ålesund,
912 Svalbard, *Atmospheric Chem. Phys.*, 13(7), 3643–3660, doi: 10.5194/acp-13-3643-2013, 2013.
- 913 Turetta, C., Feltracco, M., Barbaro, E., Spolaor, A., Barbante, C., & Gambaro, A.: A Year-Round
914 Measurement of Water-Soluble Trace and Rare Earth Elements in Arctic Aerosol: Possible Inorganic
915 Tracers of Specific Events, *Atmosphere*, 12(6), 694, doi: 10.3390/atmos12060694, 2021.
- 916 Vecchiato, M., Barbaro, E., Spolaor, A., Burgay, F., Barbante, C., Piazza, R. and Gambaro, A.,
917 Fragrances and PAHs in snow and seawater of Ny-Ålesund (Svalbard): Local and long-range
918 contamination. *Environmental Pollution* 242, 1740-1747, doi: 10.1016/j.envpol.2018.07.095, 2018.
- 919 Weingartner, E., Saathoff, H., Schnaiter, M., Streit, N., Bitnar, B. and Baltensperger, U.: Absorption of
920 light by soot particles: determination of the absorption coefficient by means of aethalometers, *J. Aerosol*
921 *Sci.*, 34(10), 1445–1463, doi:10.1016/S0021-8502(03)00359-8, 2003.
- 922 Wendl, I. A., Menking, J. A., Färber, R., Gysel, M., Kaspari, S. D., Laborde, M. J. G. and Schwikowski,
923 M.: Optimized method for black carbon analysis in ice and snow using the Single Particle Soot
924 Photometer, *Atmospheric Meas. Tech.*, 7, 2667–2681, doi:10.5194/amt-7-2667-2014, 2014.
- 925 Xu, B., T. Yao, X. Liu, and N. Wang, Elemental and organic carbon measurements with a two-step
926 heating gas chromatography system in snow samples from the Tibetan Plateau, *Ann. Glaciol.*, 43, 257–
927 262, doi: 10.3189/172756406781812122, 2006.
- 928 Yasunari, T. J., Tan, Q., Lau, K.-M., Bonasoni, P., Marinoni, A., Laj, P., Ménégos, M., Takemura, T. and
929 Chin, M.: Estimated range of black carbon dry deposition and the related snow albedo reduction over
930 Himalayan glaciers during dry pre-monsoon periods, *Atmos. Environ.*, 78, 259–267,
931 doi:10.1016/j.atmosenv.2012.03.031, 2013.
- 932 Zanatta, M., Gysel, M., Bukowiecki, N., Müller, T., Weingartner, E., Areskou, H., Fiebig, M., Yttri, K.
933 E., Mihalopoulos, N., Kouvarakis, G., Beddows, D., Harrison, R. M., Cavalli, F., Putaud, J. P., Spindler,
934 G., Wiedensohler, A., Alastuey, A., Pandolfi, M., Sellegri, K., Swietlicki, E., Jaffrezo, J. L.,
935 Baltensperger, U. and Laj, P.: A European aerosol phenomenology-5: Climatology of black carbon
936 optical properties at 9 regional background sites across Europe, *Atmos. Environ.*, 145, 346–364,
937 doi:10.1016/j.atmosenv.2016.09.035, 2016.
- 938 Zanatta, M., Laj, P., Gysel, M., Baltensperger, U., Vratolis, S., Eleftheriadis, K., Kondo, Y., Dubuisson,
939 P., Winiarek, V., Kazadzis, S., Tunved, P. and Jacobi, H.-W.: Effects of mixing state on optical and
940 radiative properties of black carbon in the European Arctic, *Atmospheric Chem. Phys.*, 18(19), 14037–
941 14057, doi: 10.5194/acp-18-14037-2018, 2018.
- 942 Zangrando, R., Barbaro, E., Zennaro, P., Rossi, S., Kehrwald, N. M., Gabrieli, J., Barbante, C. and
943 Gambaro, A.: Molecular Markers of Biomass Burning in Arctic Aerosols, *Environ. Sci. Technol.*,
944 47(15), 8565–8574, doi:10.1021/es400125r, 2013.